

Ecography

**ECOG-04028**

Dokter, A. M., Desmet, P., Spaaks, J. H., van Hoey, S., Veen, L., Verlinden, L., Nilsson, C., Haase, G., Leijnse, H., Farnsworth, A., Bouten, W. and Shamoun-Baranes, J. 2019. bioRad: biological analysis and visualization of weather radar data. – Ecography doi: 10.1111/ecog.04028

**Supplementary material**

## Appendix 1

### Calculation of vertical profiles

Vertical profiles are calculated in bioRad using the algorithm vol2bird described in Dokter et al. 2011 (C code available on Github, <https://github.com/adokter/vol2bird>). We briefly summarize the main processing steps.

1. *Precipitation cell identification: dual-polarization radar.* Meteorological signals are removed from polar scans (sweeps) based on correlation coefficient (which indicate the temporal autocorrelation of the vertically and horizontally polarized components of the detected signal by the radar), for which high values ( $>0.95$ ) is a highly reliable polarimetric indicator of precipitation (Stepanian et al. 2016). A cell-searching algorithm detects contiguous cells of high correlation coefficient, defining cells as groupings of sample volumes within an elevation scan for which each sample volume has a correlation coefficient above a threshold  $r_{ho\_hv}$  (default 0.95) and at least five directly neighboring sample volumes (in a queen or Moore neighborhood sense) that also meet this requirement.
2. *Precipitation cell identification: single-polarization radar (C-band only).* Sample volumes are grouped following a threshold in reflectivity factor ( $> 0$  dBZ) using the same cell finding criteria as above. For each cell, a cell-averaged reflectivity factor  $Z_{cell}$  and nearest neighbor radial velocity standard deviation  $\sigma_{cell}$  is calculated (see Dokter et al. 2011 for definitions) and only cells with  $\sigma_{cell} > 5 \text{ m s}^{-1}$  or  $Z_{cell} > 15$  dBZ are classified as precipitation. This approach relies on the typically low spatial variation in radial velocity and high reflectivity of precipitation relative to bird migration. The latter criteria breaks down at S-band, where reflectivity factors associated with bird

migration are higher and overlap much more with precipitation, therefore single-polarization mode is only available at C-band.

3. *Assigning precipitation and clutter masks.* Only resolution samples in precipitation cells with an area of 0.5 km<sup>2</sup> or larger are assigned to the precipitation mask, in order to retain the occasional speckle found in bird migration areas. An additional fringe of by default 5 km width around the selected precipitation cells is added to effectively remove the borders of precipitation areas, limiting the risk of precipitation contaminations. Sample volumes with a Doppler velocity in the interval of -1–1 m s<sup>-1</sup> are assigned to a second clutter mask, to filter out ground echoes associated with anomalous beam propagation (Doviak and Zrnić 1993), and clutter from other remaining static ground targets.
4. Resolution samples are grouped into height layers with a user-specified thickness, where the height  $h$  above mean sea level of a resolution sample at range  $r$  and elevation  $\theta$  is calculated by  $h = h_0 + \sqrt{r^2 + R^2 + 2rR \sin \vartheta} - R$  (Doviak and Zrnić 1993) with  $h_0$  the antenna height above mean sea level (taken from metadata of the radar volume file) and  $R = k * R_e$  the effective radius of the earth with  $R_e$  earth's radius (6371 km). We use  $k=4/3$  to account for diffraction in a standard atmosphere (Doviak and Zrnić 1993, cf. Buler and Diehl (2009) for approaches to account for refraction based on meteorological data).
5. The geometric mean of reflectivity factor values ( $Z$ ) over all resolution samples is calculated for each altitude layer excluding samples in the clutter mask, once excluding samples in precipitation mask (stored as profile quantity  $\text{eta}$  after converting the averaged reflectivity factor to reflectivity (cm<sup>2</sup>/km<sup>3</sup>)), and once including samples in the precipitation mask (stored on a dB scale as profile quantity DBZH).

6. Aliasing is the effect that radial velocities get folded to a different velocity interval when speeds exceed the Nyquist velocity of a scan, which is related to the radars pulse repetition frequency (PRF). Radial velocities are dealiased using a fit to a linear velocity model that is wrapped at the Nyquist velocity of each scan (Haase and Landelius, 2004), similar to a dealiasing technique that has been applied in bird migration studies using North-American NEXRAD radars (Sheldon et al. 2013). In vol2bird/bioRad's implementation, the samples of different elevation scans are grouped by altitude layer and de-aliased together in a single fit, taking into account each of the (potentially different) Nyquist velocities of the elevation scans.
7. Ground speeds and direction are estimated from (dealiased) radial velocity fields using the volume velocity profiling (VVP) technique (Waldteufel and Corbin 1978, Holleman 2005). In the VVP fit the radial velocity resolution samples grouped within a height layer are fit to a linear velocity model  $u \sin \phi \cos \theta + v \sin \phi \sin \theta + w \sin \theta$ , with  $\theta$  elevation,  $\phi$  azimuth,  $u$  ground speed from west to east,  $v$  ground speed from south to north,  $w$  the vertical speed. Samples in the ground clutter mask are excluded. The VVP fit is performed once excluding samples in the precipitation mask to estimate ground speed of the biological scatterers, and once including samples in the precipitation mask to obtain the radial velocity standard deviation  $sd\_vvp$  calculated from the fit residuals (Eq. A2 in Dokter et al. 2011).

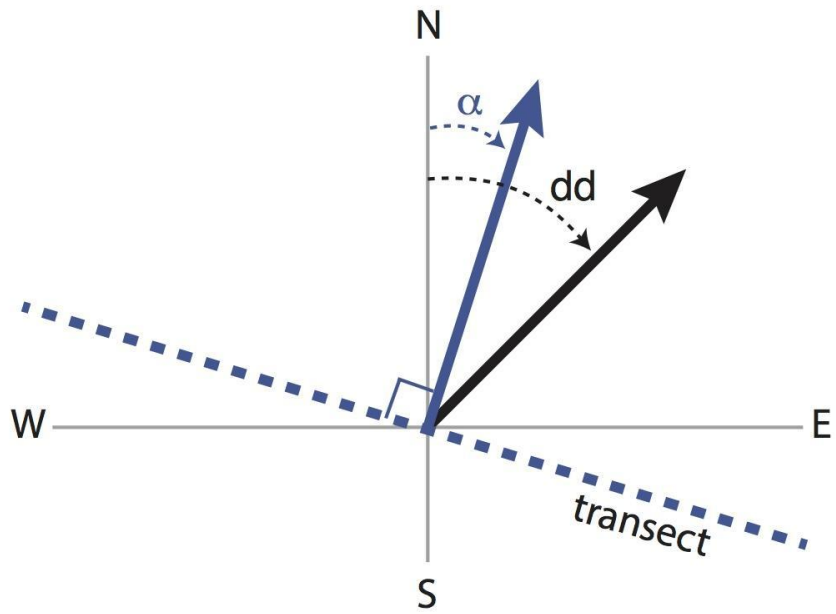


Figure A1. Ground speed direction  $dd$  and transect angle  $\alpha$  are defined clockwise relative to north. Transect orientation is defined by a vector perpendicular to the transect.

## References

Sheldon, D. et al. 2013. Approximate Bayesian inference for reconstructing velocities of migrating birds from weather radar. - Proc. AAI: 1334–1340.